



## ORIGINAL ARTICLE

# An integrated strategy by chemical characterization, *in vivo* metabolism, chemical isolation, and activity evaluation to target discovery of potential active substances in traditional Chinese medicine: *Mori Fructus* as an example



Xi-yang Tang<sup>a,1</sup>, Peng-cheng Zhao<sup>a,1</sup>, Ming-hao Chen<sup>a,1</sup>, Xiao-xing Wang<sup>a</sup>, Cai-lian Fan<sup>b,\*\*</sup>, Zhi-hong Yao<sup>a</sup>, Xin-sheng Yao<sup>a</sup>, Yi Dai<sup>a,\*</sup>

<sup>a</sup> Institute of Traditional Chinese Medicine & Natural Products, College of Pharmacy, Guangdong Province Key Laboratory of Pharmacodynamic Constituents of TCM and New Drugs Research, and International Cooperative Laboratory of Traditional Chinese Medicine Modernization and Innovative Drug Development of Ministry of Education (MOE) of China, Jinan University, Guangzhou 510632, PR China

<sup>b</sup> College of Medicine, Henan Engineering Research Center of Funiu Mountain's Medicinal Resources Utilization and Molecular Medicine, Pingdingshan University, Pingdingshan, Henan 467000, PR China

Received 9 November 2022; accepted 23 March 2023

Available online 30 March 2023

## KEYWORDS

*Mori Fructus*;  
*In vivo* metabolism;  
LC-MS guided isolation;  
Alkaloids;  
Lipid-lowering activity;  
PCSK9

**Abstract** *Mori Fructus* (MF) is a famous edible fruit of *Morus alba* L. as well as traditional Chinese medicine (TCM). Moreover, exposure behavior of complex components *in vivo* is a necessary way to elucidate active substances in TCMs. However, the effective discovery of active ingredients from MF *in vivo* is still a challenge for researchers. In this study, an integrated strategy with chemical characterization, *in vivo* metabolism, chemical isolation, and activity evaluation was established and applied in targeted discovery of potential lipid-lowering substances in MF. First, an ultra-performance liquid chromatography with quadrupole time-of-flight mass spectrometry method was established to characterize various chemical components in MF extract. Second, with the automatic matching (in-house database), discriminant ions analysis and metabolite software prediction, the metabolic profiling of different types of MF was elucidated *in vivo*. And the compounds from MF with high MS response *in vivo* were discovered. Third, according to LC-MS information of fractions, these compounds were isolated and identified by NMR. Finally, the isolated compounds were evaluated for the lipid-lowering activity on determination of triglyceride levels in high

\* Corresponding authors at: Institute of Traditional Chinese Medicine and Natural Products, College of Pharmacy, Jinan University, China.

\*\* Corresponding authors at: College of Medicine, Henan Engineering Research Center of Funiu Mountain's Medicinal Resources Utilization and Molecular Medicine, Pingdingshan University, China.

E-mail addresses: fan20094569@163.com (C.-l. Fan), daiyi1004@163.com (Y. Dai).

<sup>1</sup> These authors contributed equally to this work.

fructose-induced HepG2 cells at different concentrations. And PCSK9 inhibitory and LDL-R promoting activity were measured by western blot experiment. As a result, a total of 72 constituents were characterized in MF. After oral administration of MF extract, 16 prototypes and 33 metabolites were rapidly screened out. And the metabolism features of alkaloids, flavonols and organic acids were further revealed. Six alkaloids (morusimic acid A-D, G, F), with high MS response *in vivo* and no reference standards on the market, were isolated guided by LC-MS and identified by NMR. Among them, morusimic acid A, B, G and F could reduce triglyceride levels in fructose-induced HepG2 cells. Moreover, with western blot experiment, morusimic acid A, B, G and F could inhibit the expression of PCSK9 protein. And morusimic acid A, B and F could increase the expression of LDL-R protein. This work provides meaningful information for the discovery of potential compounds in MF for the treatment of obesity and hyperlipidemia, along with a new approach for exploring effective compounds from complex systems.

© 2023 The Author(s). Published by Elsevier B.V. on behalf of King Saud University. This is an open access article under the CC BY-NC-ND license (<http://creativecommons.org/licenses/by-nc-nd/4.0/>).

## 1. Introduction

For a long time, plant-derived traditional medicines have played an important role in preventing and treating diseases (Yuan and Lin, 2000). As we all know, the multi-functional secondary metabolites in medicinal plants are the reason for their therapeutic effects, and also the reliable source for the discovery of lead compounds (Majolo et al., 2019; Newman and Cragg, 2016). Considering its clinical application and chemical composition complexity, researchers have developed many methods to explore more potential compounds to develop drugs with efficacy (Kang et al., 2018; Setzer et al., 2000; Zhang et al., 2018a; Zhao et al., 2018). Traditionally, the method based on bioactivity directed separation and isolation can discover and characterize active ingredients in plant-derived traditional medicines (Setzer et al., 2000; Zhao et al., 2018). With the development of liquid chromatography-mass spectrometry (LC-MS), the method based on LC-MS technology guided separation and isolation combined with activity evaluation will further promote the understanding of its chemical diversity and pharmacological activities of traditional Chinese medicine (TCM) (Kang et al., 2018; Zhang et al., 2018a). In addition, it has been accepted that the pharmacodynamic effect can be produced only when the components of TCMs are absorbed into the body and reach a certain concentration (Mi et al., 2019; Zhou et al., 2014). And the *in vivo* disposal process of different structural types of components in TCM is inconsistent. Thus, the *in vivo* process of components is the key part to discover the effective substances in TCM. To sum up, it is still challenging to discover and identify the *in vivo* effective components due to the structural complexity and the different *in vivo* disposal processes of constituents from TCM. Therefore, this study proposed an integrated strategy with chemical characterization, *in vivo* metabolism, chemical isolation, and activity evaluation to rapid identify chemical components in TCM, and discover potential active substances.

*Mori Fructus* (MF), which belongs to the Moraceae family, is a famous edible fruit of *Morus alba* L. as well as Traditional Chinese Medicine (Bian et al., 2021; Chan et al., 2016; Ma et al., 2022). In recent years, many pharmaceutical studies about MF have been reported, including hypolipidemic (Zhang et al., 2019b), anti-obesity (Wu et al., 2013), antidiabetic (He et al., 2018), antioxidant (Jelled et al., 2017), and immunomodulatory (He et al., 2018). A lot of active ingredients from MF have also been investigated, covering polysaccharides, flavonoids, anthocyanins, and phenolic compounds (Bian et al., 2021; Chen et al., 2018). In addition, some research has been reported that alkaloids were one of main chemical structures in various part of *Morus alba* L. (*Mori Cortex*, *Mori Folium*, *Mori Fructus*), with promising biological activity (Asano et al., 1994; Asano et al., 2001; Cao et al., 2021; Chen et al., 2018; Kusano et al., 2002). Characteristically, 1-deoxynojirimycin, a natural piperidine alkaloid isolated from *Morus alba* L., has the inhibition of fat accumulation (Tsuduki et al., 2009). It

was reported that 1-deoxynojirimycin inhibited the accumulation of lipid by activating the hepatic fatty acid  $\beta$  oxidation system (Do et al., 2015). 1-deoxynojirimycin, as well as mulberry extracts enriched with 1-deoxynojirimycin, can also strongly inhibit hepatic triglyceride (TG) levels (Tsuduki et al., 2009). Above research indicated that there were still some compounds with excellent activity in MF, and there is an urgent need to develop a method to systematically characterize the chemical compounds in MF and screen out potential lipid-lowering substances.

In this study, in order to targeted discovery of potential lipid-lowering materials in MF, an integrated strategy with four parts was established (Fig. 1). First, the chemical components in MF were characterized by UPLC/Q-TOF MS. Second, the metabolic profiling of different types of MF was elucidated *in vivo* by the automatic matching (in-house database), discriminant ions analysis and metabolite software prediction. Third, the alkaloids with high MS response were discovered and isolated by LC-MS guided, and unambiguously identified by NMR spectral analysis. Finally, the lipid-lowering activities of the isolated alkaloids were further evaluated by *in vitro* experiments. Moreover, it has been reported that PCSK9 and LDL-R proteins are widely recognized as potential targets for the treatment of lipid disorders related diseases (Musunuru et al., 2021; Petroglou et al., 2020). Therefore, the effects of compounds on the expression of PCSK9 and LDL-R proteins were assessed. Our work provided meaningful information for revealing the potential lipid-lowering substances of MF, and new insight for exploring the effective candidates from complex systems was also supplied.

## 2. Material and methods

### 2.1. Chemicals and reagents

MF (the dried fruits of *Morus alba* L.) was supplied by Guangdong Tai'antang Pharmaceutical Co., Ltd. (Guangdong, China) and further identified by Prof. Ying Zhang in Jinan University (Guangzhou, China). Voucher specimens were deposited in the College of Pharmacy, Jinan University (Guangzhou, China). Column chromatography was undertaken with silica gel (100–200, 200–300 mesh, Qingdao Marine Chemical Ltd, China), ODS gel (12 nm, YMC Co., Ltd, Japan). TLC was carried out on silica HSGF254 (Qingdao Haiyang Chemical Co., Ltd, China). 1D and 2D NMR spectra were acquired on Bruker AV 600 (Bruker Co., Ltd, Bremen, German) using solvent signals (methanol  $d_4$  and DMSO  $d_6$ , Cambridge Isotope Laboratories, Inc., Saint Louis, USA) as internal standards. Analytical HPLC was performed on a Shimadzu HPLC system (Shimadzu, Kyoto, Japan) with an

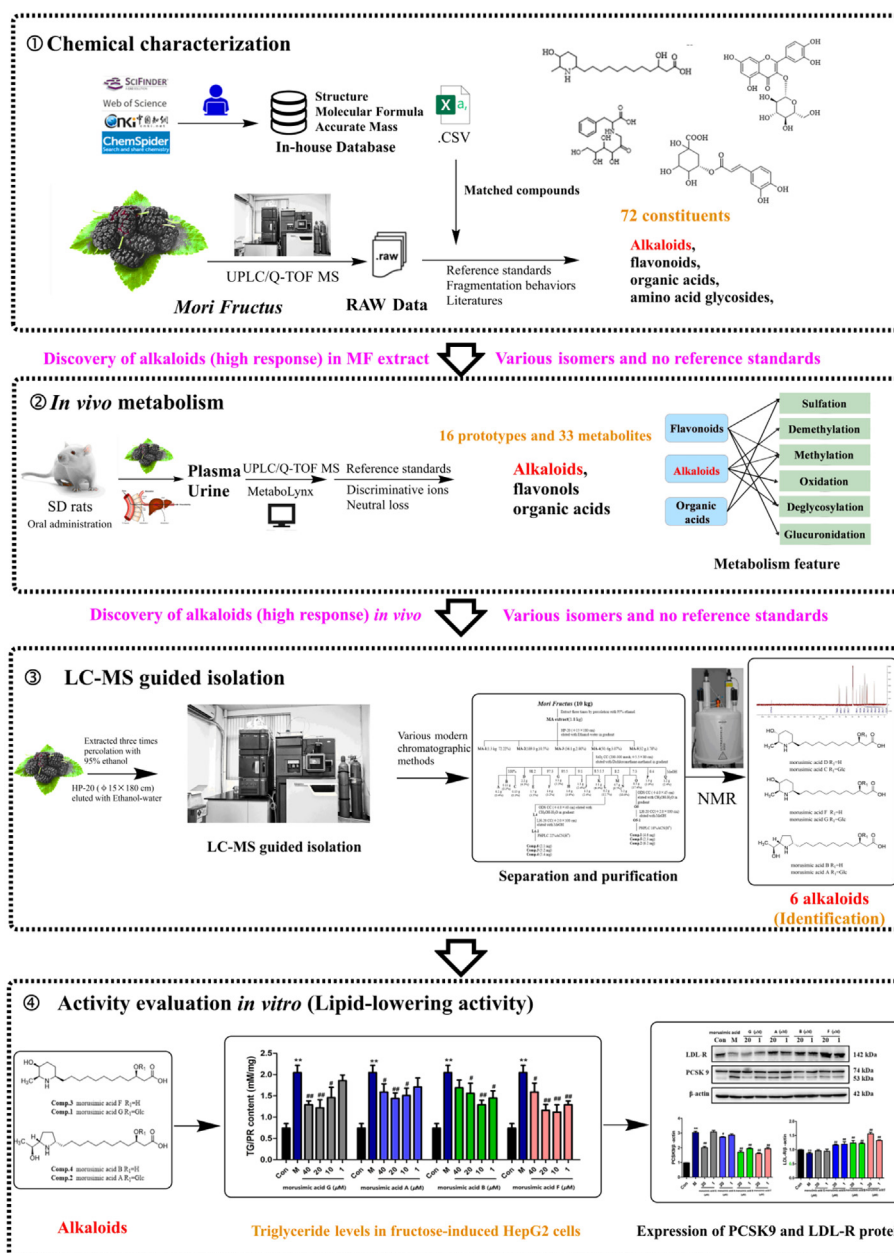


Fig. 1 The integrated strategy for target discovery of potential lipid-lowering materials in *Mori Fructus*.

LC-20AB solvent delivery system and an SPD-20A UV/vis detector using a Cosmosil 5C18-MS-II column (4.6 mm × 250 mm, 5 μm). Semi-preparative HPLC was performed on a Shimadzu HPLC system (Shimadzu, Kyoto, Japan) equipped with LC-6AD solvent delivery system and a SPD-20A UV/vis detector on a Cosmosil C<sub>18</sub> column, (10 mm × 250 mm, 5 μm).

Rutin, quercetin 3-O-glucoside, kaempferol 3-rutinoside, quercetin, kaempferol, isobavachalcone and linolenic acid were purchased from Chengdu Cromax Biotechnology Co., Ltd. (China). Protocatechuic acid, azelaic acid, chlorogenic acid, neochlorogenic acid and 3,4-dicaffeoylquinic acid was purchased from Chengdu Prefa Technology Development Co., Ltd. (China). Morusinic acid A, morusinic acid B, morusinic acid C, morusinic acid D, morusinic acid F and

morusinic acid G were isolated in author's laboratory, and were further identified by NMR spectrometry and mass spectrometry. (purity > 95%). Other chemicals and materials were all analytical grade. Other chemicals and materials were all analytical grade.

HepG2 cells (Human hepatocellular liver carcinoma cell line) were purchased from Jiangsu Kangmin Biomedical Technology Co. LTD (Jiangsu, China, batch NO: HUCL0165).

## 2.2. Sample preparation for UPLC/Q-TOF MS analysis

Dried MF (2.0 g) was cut into pieces and extracted with 20 mL of 70% (v/v) aqueous methanol for 30 min by ultrasonic

treatment at room temperature. After centrifugation at 14,000 rpm/min for 10 min, an aliquot (2  $\mu$ L) of supernatant was injected into the UPLC-Q/TOF-MS for analysis.

### 2.3. Animal and drug administration

For drug administration, MF (100 g) were extracted three times (each for 2 h) with 1000 mL of water under heating reflux. All of the extract solutions were combined and evaporated to bring the final concentration to 1.0 g/mL (equivalent to the weight of MF) at 37 °C under reduced pressure, and the extracts were then stored at -4°C before use. SPF-grade male Sprague Dawley rats (250  $\pm$  20) g were provided by Medical Laboratory Animal Center of Guangdong Province (Guangzhou, China). They were housed at ambient temperature of 24  $\pm$  2 °C with 12 h light/dark cycles for one week before experiment. During this time, a standard diet and water were freely access to rats. Before the experiment, the animals were fasted overnight with water in metabolic cages separately. After that, six rats were randomly divided into two groups: MF group ( $n = 4$ ) and blank group ( $n = 2$ ). Rats from the MF group were administrated at dosages of 15 g/kg/day for four days, and Rats from the blank group were given an equal amount of water respectively. The animal protocols were approved by the Guide for the Care and Use of Laboratory Animals of Jinan University. All procedures were in accordance with Guide for the Care and Use of Laboratory Animals (National Institutes of Health).

### 2.4. Collection and pretreatment of biological samples

After the last intragastric administration, the rats were anesthetized and blood samples were collected from the hepatic portal vein into heparinized tubes at 30, 60, 120, and 240 min after oral administration, respectively. Each group of the plasma sample was then centrifuged at 14,000 rpm/min for 10 min at 4 °C. An aliquot of 1 mL plasma was processed by 3 mL of acetonitrile to precipitate the protein. After centrifuging at 14,000 rpm for 10 min, the supernatant was dried under nitrogen gas at room temperature. The rats were housed in stainless steel metabolic cages and provided free access to water. Urine samples were collected during the periods of 0–48 h after oral administration of MF. The collected urine samples (10 mL) were directly loaded on preconditioned HLB columns (6 cc, 200 mg, Waters Oasis, Ireland), and then eluted with 12 mL of 5% methanol and 3 mL of methanol successively. The methanol eluent was collected and dried with nitrogen at room temperature. All residues were separately reconstituted in 200  $\mu$ L methanol. Aliquots of 2  $\mu$ L of the plasma and urine samples were injected into the UPLC-Q/TOF-MS.

### 2.5. UPLC/Q-TOF MS conditions

The analysis was performed on an Acquity<sup>TM</sup> UPLC I-Class system equipped with a binary solvent system, an automatic sample manager, and photodiode array detector (Waters Corporation). The chromatographic separation was achieved on an ACQUITY<sup>TM</sup> HSS T3 Column (2.1 mm  $\times$  100 mm, 1.8  $\mu$ m) at the temperature of 35 °C. The mobile phases consisted of eluent A (0.1% formic acid in water,  $v/v$ ) and eluent

B (0.1% formic acid in acetonitrile,  $v/v$ ). The solvent was delivered at a flow rate of 0.4 mL/min using a gradient elution program as follow: 0–3 min, 2–12% B; 3–9 min, 12–22% B; 9–12 min, 22–27% B; 12–15 min, 27–60% B; 15–19 min, 60–100% B; 19–21 min, 100% B; 21–21.5 min, 100–2% B; 21.5–23 min, 2% B. The injection volume was 2  $\mu$ L.

The UPLC system was coupled to a hybrid quadrupole-orthogonal time-of-flight (Q-TOF) tandem mass spectrometer equipped with electrospray ionization (SYNAPT<sup>TM</sup> G2 HDMS, Waters, Manchester, U.K.). The operating parameters were as follows: capillary voltage of 3.0 kV (ESI<sup>+</sup>) or -2.5 kV (ESI<sup>-</sup>), sample cone voltage of 35 V (ESI<sup>+</sup>) or 40 V (ESI<sup>-</sup>), source temperature of 100°C, desolvation temperature of 300°C, cone gas flow of 50 L/h, and desolvation gas flow of 800 L/h. Argon was used as collision gas for CID in both MS<sup>E</sup> and MS<sup>2</sup> mode. To ensure mass accuracy and reproducibility, the mass spectrometer was calibrated with sodium formate solution in the range of 50–1500 Da. Leucine enkephalin (positive ion mode  $m/z$  556.2771, negative ion mode  $m/z$  554.2615) was used as the LockSpray<sup>TM</sup> external reference, with a constant current of 5  $\mu$ L/min. The data was centroided during the acquisition process. Data analysis was performed by MassLynx (V4.1, Waters Corporation, Milford, MA).

### 2.6. LC-MS guided isolation of potential prototype compounds

The dried MF (10.0 kg) was extracted by percolation process with 95% ethanol. The combined ethanol extract was evaporated under reduced pressure to thick extract with no smell of alcohol. For further separation, 1.8 kg crude extract was loaded onto a column containing Diaion HP-20 resin, which was prepacked with methanol and equilibrated with distilled water, then eluted with ethanol–water in gradient (10%–100%). Finally, the enrichment of target alkaloids was obtained by LC-MS. And the target fraction MA-4 (50.1 g) was subjected to column chromatographed on a silica gel column with a gradient of CH<sub>2</sub>Cl<sub>2</sub>–MeOH to give 17 fractions (Fr. A to Fr. Q). Fr. L (6.2 g) was chromatographed on a ODS column and eluted with CH<sub>3</sub>OH–H<sub>2</sub>O. After that, Fr. L4 was separated by Sephadex LH-20 (MeOH) to yield a mixture (L4-1), and further purified by semi-preparative HPLC (C<sub>18</sub> column; 22% ACN–H<sub>2</sub>O;  $v/v$ ) to get compound 4 (2.1 mg), compound 5 (5.2 mg), compound 2 (5.4 mg). Meanwhile, Fr. O (8.5 g) was chromatographed on a ODS column and eluted with CH<sub>3</sub>OH–H<sub>2</sub>O. After that, Fr. O5 was separated by Sephadex LH-20 (MeOH) to yield a mixture (O5-1), and further purified by semi-preparative HPLC (C<sub>18</sub> column; 18% ACN–H<sub>2</sub>O;  $v/v$ ) to yield compound 6 (4.6 mg), compound 3 (2.3 mg), compound 1 (6.2 mg). (Separation flow chart was provided in Fig. S1).

### 2.7. Evaluation of lipid-lowering activities

#### 2.7.1. Cell culture

HepG2 cells were cultured in Minimum Eagle's Medium containing 10% fetal bovine serum, 1% penicillin, and streptomycin in an incubator at 37 °C with 5% CO<sub>2</sub>.

#### 2.7.2. Cell viability assay

The viability of HepG2 cells were determined by MTT (Methylthiochloroethyl Manganese Tricarbonyl). HepG2

cells were seeded into 96-well plates with the density of  $10^4$  cells/mL. After treatment with series concentrations of compounds for 24 h, 20  $\mu$ L MTT was directly added into each well and the plates were kept culturing for 4 h. The medium was removed and 150  $\mu$ L DMSO was added. Finally, the OD values of cells were determined at 490 nm on a microplate reader (BioTeck, USA).

### 2.7.3. Intracellular triglyceride (TG) Quantification

HepG2 cells with 70–80% confluence in 6 well plates were incubated in serum-free MEM + 20 mmol/L fructose and series concentrations of four main compounds, respectively, for 24 h. The cells were subjected to TG quantification as introduced by the protocol of Triglyceride Quantification Kit (Beijing Applygen Co., Ltd). Each experiment was repeated in triplicate, with duplicates each.

### 2.7.4. Detection of protein expression by western blotting

Western blot analysis was performed to evaluate the expression of Lipid-lowering associated proteins. Cells were collected, then resuspended with radio immunoprecipitation assay (RIPA) buffer supplemented with 0.1 mM PMSF protease inhibitor. The cell suspension was vortexed and lysed by ultrasound and then centrifuged at 14,000 rpm for 10 min, then the supernatant was taken. The total protein concentrations were determined by BCA protein assay kit. The same amount of proteins for each sample was loaded to 10% sodium dodecyl sulfate polyacrylamide gel electrophoresis (SDS-PAGE), and the proteins separated on the gel were transferred onto a polyvinylidene difluoride (PVDF) membrane. After blocked with 5% skim milk, the membranes were then incubated with specific primary antibodies (PCSK9; LDL-R) at 4°C overnight, followed by incubation with corresponding secondary antibodies (H + L:E030120). The protein blots were finally detected by enhanced chemiluminescence (ECL) system (1705060, Bio-Rad).

### 2.7.5. Statistical analysis

All values are expressed as mean  $\pm$  S.E.M (standard error of the mean). Statistical analysis was performed on GraphPad, version 4.00, One-way ANOVA-post hoc Tukey test (PRISM 5.0.1) were used in the statistical tests. A value of  $p < 0.05$  was considered statistically significant.

## 3. Results

### 3.1. Characterization of compounds in MF extract

In this study, our previous multi-component MS recognition method proposed (Tang et al., 2020) was applied for rapid characterization of the chemical components in MF extracts. This method is briefly described as follows: (1) an in-house chemical information database (Formula, molecular weight, reference and structure) of compounds isolated from MF was established by searching the literatures in SciFinder, CNKI, and Web of Science. Totally, 102 compounds were collected to in-house database (Table S1). Based on above in-house database, matched compounds were conducted by analyzing the elemental composition of quasi-molecular ion peak. (2) According to literature and reference standards,

chromatographic behaviors and MS characteristic fragments of various structural types were summarized. (3) A total of 72 components, including 15 alkaloids, 9 amino acid glycosides, 14 flavonoids, 25 organic acids, 7 phospholipids and 2 other type components, were unambiguously identified or tentatively characterized based on analysis of chromatographic behaviors, characteristic fragmentation patterns and self-building chemical database. The base peak intensity (BPI) chromatograms of MF extract in positive and negative ion modes were shown in Fig. 2. Table S2 listed the detailed MS fragment information of the 72 compounds.

#### 3.1.1. Alkaloids

In this work, 15 alkaloids with high MS response and various isomers were tentatively characterized in MF. Based on alkaloids from MF reported in the literature, they could be divided into pyrrole and piperidine alkaloids (Asano et al., 2001; Kusano et al., 2002). With the automatic matching (in-house database) and discriminant ions analysis, pyrrole and piperidine alkaloids with high MS response were rapidly discovered. The major MS fragmentation pathways proposed for these alkaloids were shown in Fig. S2.

Peaks **23** ( $t_R = 7.52$  min), **26** ( $t_R = 7.92$  min), **29** ( $t_R = 8.33$  min), **30** ( $t_R = 8.68$  min) and **36** ( $t_R = 9.15$  min) gave quasi-molecular ion  $[M + H]^+$  at  $m/z$  492.3172 ( $C_{24}H_{45}NO_9$ ). And it generated the characteristic product ion at  $m/z$  330.2644  $[M + H-Glc]^+$  by loss of glucose group. In addition, the product ions at  $m/z$  312.2536  $[M + H-H_2O]^+$ , 294.2431  $[M + H-2H_2O]^+$ , 276.2328  $[M + H-3H_2O]^+$ , 268.2639  $[M + H-H_2O-CO_2]^+$  and 250.2534  $[M + H-2H_2O-CO_2]^+$  were further generated by losses of  $H_2O$  (18 Da) and  $CO_2$  (44 Da). According to literature and isolated standards, they were identified as morusimic acids with glucose (alkaloids) (Table S2). Peak **44** exhibited  $[M + H]^+$  at  $m/z$  330.2641, which was determined to be  $C_{18}H_{35}NO_4$ . Based on high-collision-energy scan spectra  $m/z$  328.2492 and fragment ions at  $m/z$  312.2545  $[M + H-H_2O]^+$ , the characteristic ions at  $m/z$  294.2433, 276.2292, 268.2632, 250.2542 were produced. Therefore, it was tentatively identified as morusimic acid B by searching in-house database. Furthermore, the proposed MS fragmentation pathway of Peak **44** was shown in Fig. S3. As shown in Fig S2, other alkaloids were rapidly characterized by analyzing neutral losses (162/44/18 Da) and characteristic ions ( $m/z$  330 and  $m/z$  250).

#### 3.1.2. Amino acid glycosides

In this study, a total of 9 amino acid glycosides were discovered and tentatively identified in MF. The structure of these compounds was composed of amino acid and fructose. The major MS fragmentation pathways proposed for amino acid glycosides were shown in Fig. S4. For example, peak **12** showed the quasi-molecular ions  $[M + H]^+$  at  $m/z$  328.1400 and  $[M-H]^-$  at  $m/z$  326.1244, which was determined to be  $C_{15}H_{21}NO_7$ . In the negative ion mode, the main MS fragment ion at  $m/z$  164.0727  $[M-H-Fru]^-$  corresponded to the loss of fructose. Moreover, in the positive ion mode, the  $m/z$  310.1305  $[M + H-H_2O]^+$ , 292.1160  $[M + H-2H_2O]^+$ , 264.1226  $[M + H-2H_2O-CO]^+$  and 246.1112  $[M + H-3H_2O-CO]^+$  corresponded to continuous loss of  $H_2O$  and CO at the fructose group. As the results, peak **12** was tentatively identified as

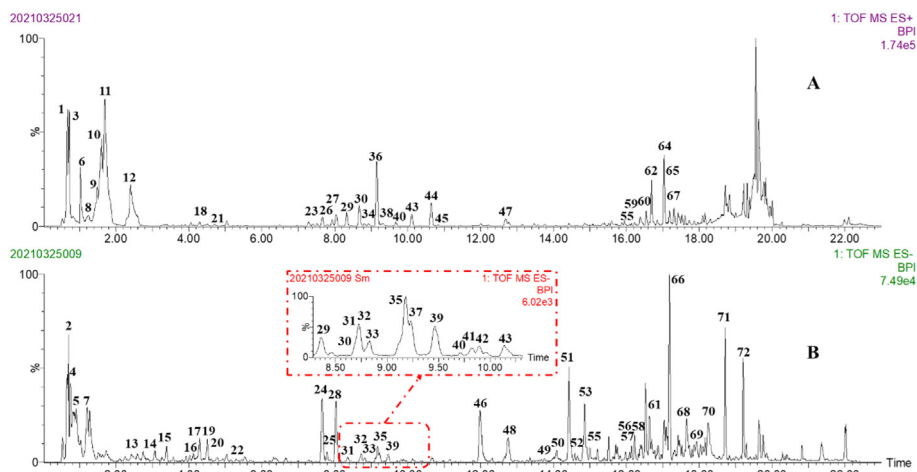


**Fig. 2** The base peak intensity (BPI) chromatograms of MF by UPLC/Q-TOF MS. (A) positive ion mode; (B) negative ion mode.

Fructose-phenylalanine. Furthermore, the proposed MS fragmentation pathway for peak **12** was shown in [Fig. S5](#).

### 3.1.3. Flavonoids

A total of 14 flavonoids were detected in MF extract. They could be classified into three sub-categories, such as flavonols, flavonones and chalcones. The main MS fragmentation information of flavonols was shown in [Fig. S6](#). Peak **48** presented a precursor ion  $[M-H]^-$  at  $m/z$  301.0350 ( $C_{15}H_{10}O_7$ ) and produced characteristic fragment ions at  $m/z$  178.9970, 151.0038 and 121.0298. Based on comparison with reference standard, it was identified as Quercetin. Peak **28** generated a precursor ion  $[M-H]^-$  at  $m/z$  463.0883 ( $C_{21}H_{20}O_{12}$ ) and produced characteristic fragment ion at  $m/z$  301.0332 by loss of glucose. The other produced ions at  $m/z$  151.0032 and 149.0244 were generated *via* RDA reaction. Thus, peak **28** was identified as quercetin 3-O-glucoside by comparison with reference standard. In addition, the MS proposed fragmentation pathways for Peak **28** were shown in [Fig. S7](#). Peak **61** presented  $[M + H]^+$  at  $m/z$  325.1436 ( $C_{20}H_{20}O_4$ ). The characteristic ion at  $m/z$  269.0808  $[M + H-C_4H_8]^+$  by cleavage of isopentene group. The other fragment ions at  $m/z$  205.0872 and 149.0250 could be obtained by RDA cleavage from the C-ring. Therefore, it was unambiguously identified as isobavachalcone by comparison with the reference standard.

### 3.1.4. Organic acids

According to the in-house database of MF, it was found that there were abundant caffeoylquinic acid in MF. In total, 25 organic acids were characterized. For example, peaks **15/17/19** gave the same precursor ion  $[M-H]^-$  at  $m/z$  353.0873, and their empirical molecular formulas were all supposed as  $C_{16}H_{18}O_9$ , which further fragmented to afford the characteristic ion at  $m/z$  191.0566 [quinic acid- $H$ ], 173.0454 [quinic acid- $H-H_2O$ ], 179.0350 [caffeic acid- $H$ ], 161.0237 [caffeic acid- $H-H_2O$ ] and 135.0460 [caffeic acid- $H-CO_2$ ] in high-collision-energy scan ([Fig. S8](#)). Therefore, according to the oil-water partition coefficient and reference standards, peaks **15** (ClogP = -1.88), **17** (ClogP = -1.88) and **19** (ClogP = -1.40) were identified as 3-O-caffeoylquinic acid, 5-O-caffeoylquinic acid and 4-O-caffeoylquinic acid, respectively.

## 3.2. Metabolic profiling of MF in rat plasma and urine

In total, 16 prototypes (including 10 alkaloids, 2 flavonols and 4 organic acids) and 33 metabolites (including 8 alkaloids, 19 flavonols and 6 organic acids) were rapidly screened out after the oral administration of MF. Due to the high MS response of alkaloids and other components at 0.5 h plasma, the time point of 0.5 h was finally selected for figure display. Extracted ion chromatograms (EICs) of prototypes and metabolites for drugged plasma and urine samples were shown in [Fig. 3](#) and [Fig S9](#). It is worth noting that many alkaloids (**P4** ~ **P8**, **P10** ~ **P13**) had high MS response *in vivo*, which indicated that such components might be the key effective substances of MF to play its role.

### 3.2.1. Identification of prototype components in rat bio-samples

Based on self-database, retention times, quasi-molecular ions and characteristic fragment ions from chemical constituents of MF, 16 prototypes were rapidly screened out. The detailed MS fragmentation information was shown in [Table 1](#) and Extracted ion chromatograms (EICs) of prototypes for drugged plasma and urine samples were shown in [Fig. 3](#). Furthermore, it was found that the alkaloids had high response *in vivo*, but the structure of them cannot be determined because many isomers and no reference standards.

### 3.2.2. Identification of metabolites in rat plasma and urine

As a result, 33 metabolites were detected in rat plasma and urine. And its main metabolic features included oxidation, deglycosylation, methylation, demethylation glucuronidation and sulfation. According to the origins of prototypes and mother nuclear structures (caffeoylquinic acid, caffeic acid, morusimic acid A-G, quercetin, Kaempferol, etc.), we screened the potential metabolites *in vivo* by MDF technique-based data processing, and it was operated on MetaboLynx XS software. The related detailed information of metabolites was shown in [Table S3](#).

**3.2.2.1. Alkaloid-related metabolites.** It was the first time to characterize the metabolism feature of the alkaloids in MF. 8 alkaloid-related metabolites were identified in rat urine and

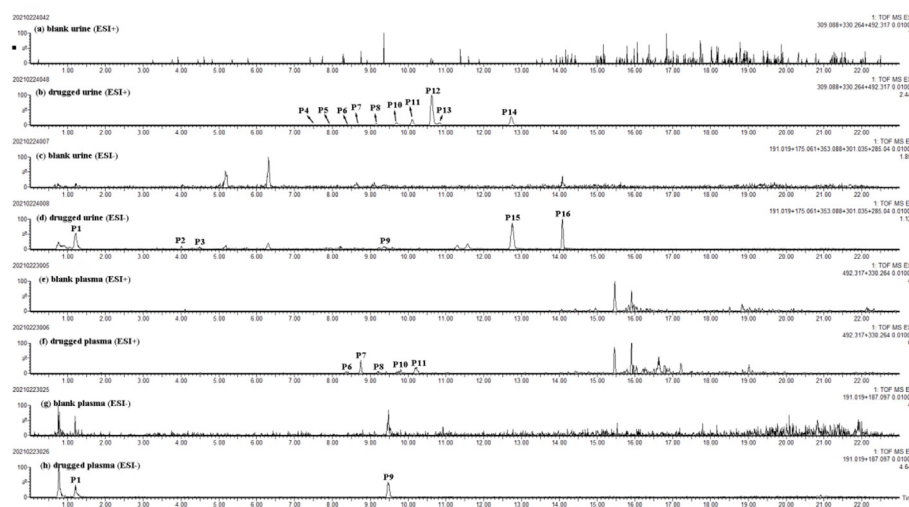


**Fig. 3** Extracted ion chromatograms (EICs) of prototypes in blank and drugged biosamples. (a) blank urine in positive mode; (b) drugged urine in positive mode; (c) blank urine in negative mode; (d) drugged urine in negative mode; (e) blank plasma in positive mode; (f) drugged plasma in positive mode; (g) blank plasma in negative mode; (h) drugged plasma in negative mode.

**Table 1** UPLC/Q-TOF MS information of prototypes in rat plasma and urine.

NO.	$t_R$ (min)	Formula	Selected ion	Measured mass	MS fragments	Identification	Source (biological)
P1	1.21	$C_6H_8O_7$	$[M-H]^-$	191.0191 (-0.3)	111.0089	Citric acid	P,U
P2	4.03	$C_7H_{12}O_5$	$[M-H]^-$	175.0611 (0.5)	<b>131.0697</b>	Malic acid	U
P3	4.48	$C_{16}H_{18}O_9$	$[M-H]^-$	353.0884 (1.1)	<b>191.0548</b> , 179.0346	Cryptochlorogenic acid	U
P4	7.52	$C_{24}H_{45}NO_9$	$[M + H]^+$	492.3182 (0.9)	474.3057	Morusimic acid C isomer I	U
P5	7.94	$C_{24}H_{45}NO_9$	$[M + H]^+$	492.3173 (0.0)	474.2973	Morusimic acid C isomer II	U
P6*	8.34	$C_{24}H_{45}NO_9$	$[M + H]^+$	492.3171 (-0.2)	474.3091, 312.2500, 268.2639, <b>250.2543</b>	Morusimic acid C	P,U
P7*	8.69	$C_{24}H_{45}NO_9$	$[M + H]^+$	492.3186 (1.3)	<b>330.2673</b> , 312.2518, <b>250.2523</b>	Morusimic acid G	P,U
P8*	9.16	$C_{24}H_{45}NO_9$	$[M + H]^+$	492.3181 (0.8)	474.3039, <b>330.2629</b> , 312.2543, 276.2332, <b>250.2539</b>	Morusimic acid A	P,U
P9	9.47	$C_9H_{16}O_4$	$[M-H]^-$	187.0972 (0.2)	125.0967	Azelaic acid	P,U
P10*	9.71	$C_{18}H_{35}NO_4$	$[M + H]^+$	330.2649 (0.5)	312.2519, 276.2325, 268.2649, <b>250.2537</b>	Morusimic acid D	P,U
P11*	10.13	$C_{18}H_{35}NO_4$	$[M + H]^+$	330.2648 (0.4)	312.2538, 294.2442, 276.2325, 268.2644, <b>250.2540</b>	Morusimic acid F	P,U
P12*	10.66	$C_{18}H_{35}NO_4$	$[M + H]^+$	330.2644 (0.0)	312.2535, 294.2425, 276.2330, 268.2641, <b>250.2535</b>	Morusimic acid B	U
P13	10.84	$C_{18}H_{35}NO_4$	$[M + H]^+$	330.2646 (0.2)	312.2530, 294.2449, 276.2330, 268.2638, <b>250.2539</b>	Morusimic acid B isomer I	U
P14	12.69	$C_{17}H_{12}N_2O_4$	$[M + H]^+$	309.0872 (-0.3)	206.0844, 180.0810	Flazin	U
P15	12.76	$C_{15}H_{10}O_7$	$[M-H]^-$	301.0343 (-0.5)	151.0037	Quercetin	U
P16	14.08	$C_{15}H_{10}O_6$	$[M-H]^-$	285.0397 (-0.2)	N/A	Kaempferol	U

\* Compared with isolated standard.

P: Plasma, U: Urine.

plasma by compared with discriminant ions and neutral loss. In alkaloids, demethylation, methylation and oxidation were the main metabolic reactions *in vivo*.

**M28**, **M29**, **M30** and **M31** had the same quasi-molecular ion at  $m/z$  344.28 in the positive ion mode, which was 14 Da ( $CH_2$ ) higher than that of morusimic acid B/D/F, and it was inferred to be methylated morusimic acid B/D/F. **M4** and **M5** displayed the same molecular ion of  $[M + H]^+$  at  $m/z$

346.26 with formula as  $C_{18}H_{35}NO_5$  and showed a neutral addition of 16 Da (O) than that of morusimic acid B/D/F. They all yielded the typical fragment ion at  $m/z$  328.35, 310.24 and 248.24. Accordingly, **M4** and **M5** were identified as oxidation product of morusimic acid B/D/F. **M16** and **M19** both showed the quasi-molecular ion at  $m/z$  316.25, 14 Da ( $CH_2$ ) less than that of morusimic acid B/D/F, and it was inferred to be demethylated morusimic acid B/D/F.

**3.2.2.2. Flavonol-related metabolites.** As a result, a total of 19 flavonol-related metabolites were characterized in rat urine and plasma by comparison with MS fragment pattern and the reference literature (Hong and Mitchell, 2004; Wu et al., 2017). In MF extract, the rich flavonol-glycosides (rutin, quercetin 3-O-glucoside, etc.) could be converted into aglycone *in vivo* (quercetin) (Ou-yang et al., 2013). Therefore, aglycone was selected as parent nuclear component for metabolite analysis. And methylation, deglycosylation, glucuronidation and sulfation were main metabolic reactions *in vivo*.

**M17, M18 and M24** gave the same quasi-molecular ion at  $m/z$  477.06, which was 176 Da (GluA) higher than that of quercetin. The main fragment ion of  $m/z$  301.03 was generated by loss of a GluA group. Thus, they were identified as a glucuronidation product of quercetin. **M27** exhibited precursor ions  $[M-H]^-$  at  $m/z$  380.99, with a molecular formula of  $C_{15}H_{10}O_{10}S$ , which was one molecule of  $SO_3$  (80 Da) more than quercetin. And the characteristic fragment ion at  $m/z$  301.0354 produced by loss of a  $SO_3$  group. Therefore, it was inferred that **M48** is a sulfation product of quercetin. In addition, according to the MS characteristic fragments ions (Fig. S6) and literature (Wu et al., 2017), other flavonol-related metabolites were tentatively identified.

**3.2.2.3. Organic acids-related metabolites.** Based on discriminant ions analysis of caffeoylquinic acid and literature (Zhang et al., 2021), 6 organic acids-related metabolites were detected in rat urine and plasma after oral administration of MF extract. And organic acids mainly underwent metabolic reactions such as methylation and sulfation *in vivo*.

**M2, M8 and M11** all exhibited precursor ions  $[M-H]^-$  at  $m/z$  367.10, with a molecular formula of  $C_{17}H_{20}O_9$ , which was 14 Da more than caffeoylquinic acid (mother nuclear structures). The fragment ions at  $m/z$  193.05 and  $m/z$  191.05 (quinic acid) could be observed. It was speculated that **M2, M8 and M11** were identified as the methylation products of caffeoylquinic acid. **M1** gave the quasi-molecular ion at  $m/z$  258.99 ( $C_9H_8O_7S$ ), which was 80 Da ( $SO_3$ ) higher than that of caffeic acid. The main fragment ion at  $m/z$  179.03 was produced by loss of  $SO_3$  group. Therefore, it was inferred that **M1** was identified as the sulfation product of caffeic acid. **M3 and M13** gave the same quasi-molecular ion at  $m/z$  273.01 ( $C_{10}H_{10}O_7S$ ), which was 14 Da more than **M1**. The characteristic fragment ion at  $m/z$  193.05 was yielded. Then, **M3 and M13** were characterized as the methylation and sulfation products of caffeic acid.

### 3.3. LC-MS guided isolation and identification of alkaloids

Through chemical characterization and *in vivo* component analysis, the alkaloids were found. Due to the existence of isomers and the absence of reference materials on the market, the structure of these alkaloids cannot be confirmed. Therefore, according to the mass spectrum information of fractions, 6 alkaloids were obtained by targeted separation and purification, included morusimic acid A (**1**), morusimic acid B (**2**), morusimic acid C (**3**), morusimic acid D (**4**), morusimic acid F (**5**), morusimic acid G (**6**) (Fig. 4). And the  $^1H$  and  $^{13}C$  NMR data of 6 alkaloids were shown in Table 2.

Morusimic acid D (**4**) was obtained as a yellow powder, which showed a brownish spot on TLC by ninhydrin reaction. The molecular formula was determined to be  $C_{18}H_{35}NO_4$  on the basis of the HR-ESI-MS ( $m/z$  330.2641,  $[M + H]^+$ ), and 2 degrees of the unsaturation were determined. The  $^1H$  NMR data (Table 2) of **4** showed diagnostic signals of two hydrogen signal on carbon with oxygen [ $\delta_H$  3.96 (1H, m, H-3), and 3.37 (1H, m, H-4')], two hydrogen signal on carbon with nitrogen [ $\delta_H$  3.07 (1H, m, H-1'), 2.92 (1H, m, H-5')], and one hydrogen signal on methyl [ $\delta_H$  (1.39, 3H, d,  $J = 6.5$  Hz,  $-CH_3$ )]. In addition, there were multiple stacked proton signals near 1.3 ppm, suggesting that longer fatty chains might be present in the structure. The  $^{13}C$  NMR data showed 18 carbon signals (Table 2). Combined with the DEPT-135 experiment, these carbons could be categorized into one methyl carbon signal ( $\delta_C$  15.9), twelve methylene carbon signals ( $\delta_C$  26.3, 26.6, 28.2, 30.4, 30.4, 30.5, 30.6, 30.6, 32.8, 34.7, 38.1, 43.3), four methyne carbon signals ( $\delta_C$  58.3, 59.1, 69.3, 70.8) and one carbonyl signal ( $\delta_C$  175.8). As illustrated in Fig. S40, the  $^1H-^1H$  COSY correlation of H-1'/H-2'/H-3'/H-4'/H-5'/H(- $CH_3$ ) combined with HMBC correlations of H-5' to C-1' demonstrated the presence of piperidine ring (fragment A). Furthermore, the  $^1H-^1H$  COSY correlation of H-2'/H-3'/H-4' combined with HMBC correlations of H-3 to C-1 and H-2 to C-4 demonstrated the presence of fragment B. Further, according to the element composition, the above two fragments were removed, leaving 8 carbons and 16 hydrogens. Combined with the obvious methylene overlapping signals on the hydrogen spectrum, it was speculated that the structure existed a fat chain (fragment C). The HMBC correlations between H-2' to C-12, demonstrated that the linkage of piperidine ring and fat chain on C-2'. The HMBC correlations between H-3 to C-5, it was deduced that the linkage of

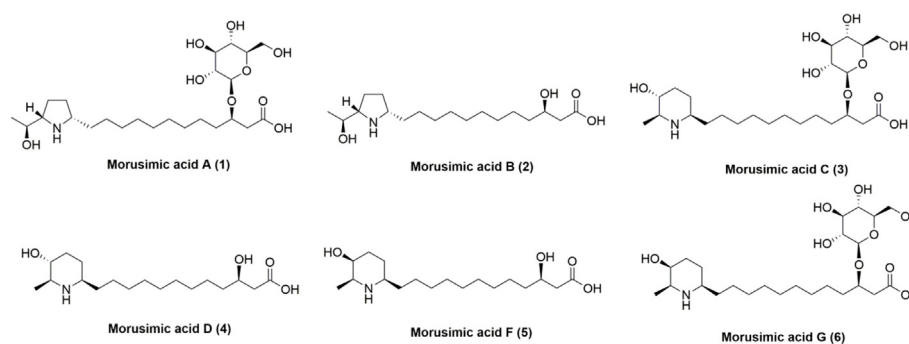


Fig. 4 Structure of 6 isolated alkaloids.

**Table 2** The  $^1\text{H}$  and  $^{13}\text{C}$  NMR data of 6 alkaloids.

Pos.	1 <sup>a</sup>		2 <sup>a</sup>		3 <sup>a</sup>		4 <sup>a</sup>		5 <sup>a</sup>		6 <sup>a</sup>	
	$\delta_{\text{C}}$	$\delta_{\text{H}}$ (J in Hz)										
1	175.8	–	175.7	–	175.6	–	175.8	–	175.6	–	175.7	–
2	40.4	2.61, dd (15.6, 6.2) 2.50, dd (15.6, 6.2)	43.3	2.37, dd (15.2, 8.1) 2.44, dd (15.2, 4.9)	40.3	2.61, dd (15.6, 6.2) 2.50, dd (15.6, 6.2)	43.3	2.37, dd (15.2, 8.1) 2.44, dd (15.2, 4.9)	43.3	2.37, dd (15.2, 8.2) 2.44, dd (15.2, 4.8)	40.3	2.61, dd (15.4, 6.2) 2.50, dd (15.4, 6.2)
3	77.3	4.12	69.3	3.96	77.2	4.12, q (6.2)	69.3	3.96	69.3	3.97	77.3	4.12, q (6.2)
4	36.1	–	38.1	1.47	36.1	1.66	38.1	1.48	38.1	1.46	36.1	1.65
5	27.8	1.42	26.6,	1.31–1.47	26.1	1.41	26.6	1.46	26.6	1.46	26.3	1.41
6	26.1	1.41	27.7,		26.4	1.41	26.3	1.46	26.3	1.37	26.1	1.41
7–	30.4, 30.4,	1.31–1.37	30.4, 30.4,		30.4, 30.4,	1.31–1.37	30.4, 30.4,	1.30–1.37	30.4, 30.4,	1.30–1.34	30.4, 30.4,	1.31–1.37
11	30.5, 30.5, 30.6		30.5, 30.6, 30.6		30.5, 30.6, 30.6		30.5, 30.6, 30.6		30.5, 30.6, 30.6		30.5, 30.6, 30.6	
12	32.9	1.67, 1.77	32.9	1.66, 1.77	34.3	1.48, 1.66	34.7	1.52, 1.66	34.7	1.55, 1.67	34.8	1.51, 1.62
1'	62.6	3.5	62.6	3.5	58.3	3.07	58.3	3.07	58.7	3.05	58.7	3.05
2'	30.6	1.67, 2.20	30.6	1.68, 2.20	28.2	1.43, 2.09	28.2	1.43, 2.08	23.6	1.70, 1.80	23.6	1.64, 1.72
3'	23.6	2.04	23.6	2.04	32.8	1.43, 2.11	32.8	1.51, 2.11	31	1.72, 1.95	31	1.65, 1.95
4'	66	3.54	66	3.53	70.8	3.39	70.8	3.37	65.8	3.84	65.8	3.8
5'	–	–	–	–	59.1	2.93	59.1	2.92	57.5	3.23	57.5	3.15
CH <sub>3</sub>	–	–	–	–	15.9	1.39, d (6.5)	15.9	1.39	15.9	1.31	15.9	1.31, d (6.5)
1''	66.1	4	66.1	3.99	–	–	–	–	–	–	–	–
2''	20.5	1.23, d (6.4)	20.5	1.23, d (6.4)	–	–	–	–	–	–	–	–
1'''	103.3	4.39, d (7.8)	–	–	103.3	4.39, d (7.8)	–	–	–	–	103.3	4.39, d (7.8)
2'''	75.3	3.15, dd (7.8, 8.9)	–	–	75.3	3.15, dd (7.8, 8.9)	–	–	–	–	75.3	3.15, dd (7.8, 8.9)
3'''	78	3.36	–	–	78	3.36, t (8.9)	–	–	–	–	78	3.36, t (8.9)
4'''	71.7	3.3	–	–	71.7	3.3	–	–	–	–	71.7	3.3
5'''	77.9	3.27	–	–	77.9	3.27	–	–	–	–	77.9	3.27
6'''	62.9	3.68, dd (11.3, 6.1) 3.85, dd (11.3, 2.0)	–	–	62.9	3.68, dd (11.3, 6.1) 3.85, dd (11.3, 2.0)	–	–	–	–	62.9	3.68, dd (11.3, 6.1) 3.85, dd (11.3, 2.0)

a: NMR data of 6 alkaloids in CD<sub>3</sub>OD.

fragment B and fragment C on C-3. Based on reported NMR spectroscopic data (Kusano et al., 2002), combined with ROESY correlations between H-1' with H-3', H-5' with H-3' and H-2' with H-4', compound 4 was elucidated as morusimic acid D.

Morusimic acid G (6) was obtained as a yellow powder, which showed a brownish spot on TLC by ninhydrin reaction. The molecular formula was determined to be C<sub>24</sub>H<sub>45</sub>NO<sub>9</sub> on the basis of the HR-ESI-MS (*m/z* 492.3162, [M + H]<sup>+</sup>), and 3 degrees of the unsaturation were determined. The <sup>1</sup>H NMR data (Table 2) of 6 showed an anomeric proton [ $\delta_{\text{H}}$  4.39 (1H, d, *J* = 7.8 Hz, H-1'''), diagnostic signals of two hydrogen signal on carbon with oxygen [ $\delta_{\text{H}}$  4.12 (1H, q, *J* = 6.2 Hz, H-3), and 3.39 (1H, m, H-4')], two hydrogen signal on carbon with nitrogen [ $\delta_{\text{H}}$  3.07 (1H, m, H-1'), 2.93 (1H, m, H-5')], and one hydrogen signal on methyl [ $\delta_{\text{H}}$  (1.39, 3H, d, *J* = 6.5 Hz, -CH<sub>3</sub>)]. In addition, there were multiple stacked proton signals near 1.3 ppm, suggesting that longer fatty chains might be present in the structure. The <sup>13</sup>C NMR data showed 24 carbon signals (Table 2). Combined with the DEPT-135 experiment, these carbons could be categorized into one methyl carbon signal ( $\delta_{\text{C}}$  15.9), thirteen methylene carbon signals ( $\delta_{\text{C}}$  23.6, 26.1, 26.3, 30.4, 30.4, 30.5, 30.6, 30.6, 31.0, 34.8, 36.1, 40.3, 62.9), nine methyne carbon signals ( $\delta_{\text{C}}$  57.5, 58.7, 65.8, 71.7, 75.3, 77.3, 77.9, 78.0, 103.3) and one carbonyl signal ( $\delta_{\text{C}}$  175.9). Signals at  $\delta_{\text{H}}/\delta_{\text{C}}$  [ $\delta_{\text{H}}$  4.39 (1H, d, *J* = 7.8 Hz, H-1''')/103.3 (C-1''') and other oxygenated methine signals revealed the presence of sugar residual. Except for the NMR data of the sugar part, the other parts are similar to compound 5. The HMBC correlations between H-1''' to C-3, demonstrated that the linkage of fat chain and glucose on C-3. In the ROSEY spectrum, no correlation between H-2' and H-4' was observed, suggesting that the orientation of H-4' in the conformation changed. Compared with reported NMR data of 3 and 5 (Kusano et al., 2002), compound 6 was tentatively identified as (3*R*)-3-hydroxy-12-[(1*R*,4*S*,5*S*)-4-hydroxy-5-methyl-piperidin-1-yl]-dodecanoic acid-3-*O*- $\beta$ -D-glucopyranoside.

Compared with NMR spectroscopic data (CD<sub>3</sub>OD) of other 4 known compounds in the literature (Kusano et al., 2002) (Table 2), compounds 1, 2, 3 and 5 were identified as morusimic acid A, morusimic acid B, morusimic acid C, morusimic acid F and morusimic acid G, respectively.

For chemical characterization and *in vivo* metabolism, peak 29 (prototype 6), peak 30 (prototype 7), peak 36 (prototype 8), peak 40 (prototype 10), peak 43 (prototype 11) and peak 44 (prototype 12) were undoubtedly identified as morusimic acid C, morusimic acid G, morusimic acid A, morusimic acid D, morusimic acid F and morusimic acid B by compared with isolated compounds, respectively.

### 3.4. Lipid-lowering effects of four alkaloids

Many active alkaloids from natural products were reported to have lipid-lowering activities (Hou et al., 2021; Song and Jiang, 2017). In addition, pharmacological studies have shown that MF has significant lipid-lowering activity (Ou et al., 2011; Wu et al., 2013). Morusimic acid A, morusimic acid B, morusimic acid F and morusimic acid G were the main alkaloids with high MS response *in vivo*. Thus, they were evaluated for their lipid-lowering activities on triglyceride levels in fructose-induced HepG2 cells. And PCSK9 and LDL-R are widely recognized as potential targets for the treatment of lipid disorders related diseases (Musunuru et al., 2021; Petroglou et al., 2020). Therefore, the effects of four alkaloids on expression of PCSK9 and LDL-R in fructose-stimulated human hepatocellular liver carcinoma cell line (HepG2) were also investigated.

#### 3.4.1. Effects of four alkaloids on triglyceride levels in high-fructose-induced HepG2 cells

To ascertain whether four alkaloids exerted cytotoxicity on HepG2 cells, MTT assay was performed. No significant toxicity was observed at the concentration range of 1–100  $\mu$ M for 24 h (Fig. S41).

As shown in Fig. 5, morusimic acid A (1), morusimic acid B (2), morusimic acid F (5) and morusimic acid G (6) could decrease triglyceride levels in high-fructose-induced HepG2 cells at the concentration range of 10 to 40  $\mu$ M, 1 to 20  $\mu$ M, 1 to 40  $\mu$ M and 10 to 40  $\mu$ M, respectively.

#### 3.4.2. Effects of four alkaloids on expression of PCSK9 and LDL-R in high-fructose-induced HepG2 cells

To further illuminate the lipid-lowering effects of the alkaloids, the expression of PCSK9 and LDL-R was investigated by

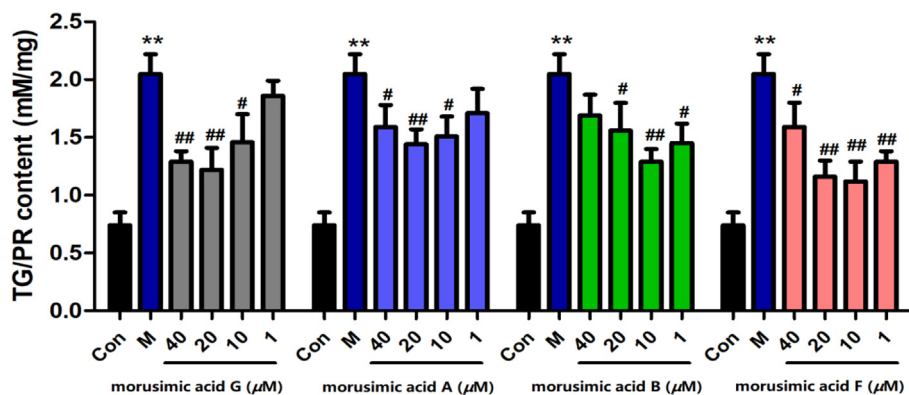


**Fig. 5** Effects of morusimic acid G, morusimic acid A, morusimic acid B and morusimic acid F on triglyceride levels in fructose-induced HepG2 cells at different concentrations (*n* = 3). \*\**P* < 0.01 vs. control group and ###*P* < 0.01, #*P* < 0.05 vs. Model group.

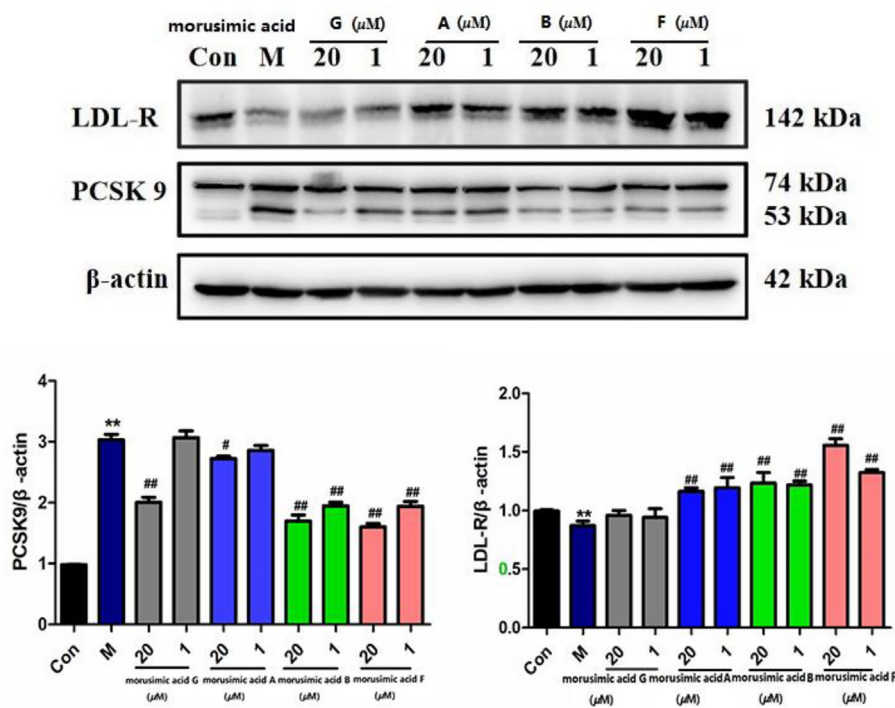


**Fig. 6** Effects of morusimic acid G, morusimic acid A, morusimic acid B and morusimic acid F on the expression of PCSK9 and LDL-R proteins at different concentrations. Protein expression was studied by western blotting with β-actin used as control (n = 3). \*\* $P < 0.01$  vs. control group and ## $P < 0.01$ , # $P < 0.05$  vs. Model group.

western blot. As shown in Fig. 6, it was demonstrated that four alkaloids could significantly inhibit the expression of PCSK9 protein at the concentration of 20 μM, especially for 2 and 5, whose inhibition rate reached to 55.9% and 52.7%. Compounds 2 (64.3%) and 5 (63.3%) with the common feature of no glucose group, also showed significant inhibitory activity at the concentration of 1 μM, indicating a decisive role in PCSK9 protein expression of 3-O-glucose group. And compounds 1, 2 and 5 could obviously increase the expression of LDL-R at 1 μM and 20 μM. To sum up, it was concluded that 1 μM of morusimic acid B (2) and morusimic acid F (5) could decrease triglyceride levels in high-fructose-induced HepG2 cells, significantly inhibit the expression of PCSK9 protein and increase LDL-R protein. Therefore, follow-up research on pharmacological mechanisms and new drug development should pay more attention to these compounds.

#### 4. Discussion

The classical approach to the discovery of active substances in natural medicines is to extract and isolate TCMs and then screen the active ingredients according to their traditional efficacy until a single component with significant activity is identified, such as artemisinin in *Artemisia annua* (Czechowski et al., 2020) and paclitaxel in *Taxus chinensis* (Wani et al., 1971). However, this method is often time-consuming and laborious, and it is easy to lose the substances that really play a role *in vivo*. Moreover, based on the viewpoint of serum pharmacology, there is a correlation between *in vivo* exposure and bioactivity of the components in TCMs (Zhang et al., 2019a). And it further effectively narrows the range of active ingredients in TCMs. Therefore, in order to effectively

identify bioactive components *in vivo*, the present strategy is combined with *in vivo* metabolism studies. In recent years, it has been reported that the bioactive compounds of MF are mainly flavonoids and phenolic acids (Du et al., 2019; Yuan and Zhao, 2017). Interestingly, except for flavonoids and phenolic acids, alkaloids were discovered and identified by using this integrated strategy in this study. This result further broadens the knowledge of the *in vivo* effective substances in MF.

In quality control of TCMs, the selection of Q-markers should focus on production and *in vivo* process based on specificity of the ingredients with the core of component-efficacy (Yang et al., 2017; Zhang et al., 2018b). In our study, further investigation suggested that morusimic acids (alkaloids) were prevalent in many batches (Table S4) of commercial MF from different origins (Fig. S42). The total content of all these alkaloids was found to be approximately 3 mg/kg in MF. As these alkaloids were dominant absorbable ingredients *in vivo* and showed lipid-lowering activity, which correlated with the effects of MF in the treatment of obesity and hyperlipidaemia (Lim and Choi, 2019), it seemed that alkaloids are important beneficial components in MF, and should be given more attention in the quality control of MF.

It is worth noting that 1-deoxynobinomycin, the main bioactive alkaloid from *Morus alba* L, was not detected in this study. According to the literature, this phenomenon may be caused by its abundance only in the roots and leaves of *Morus alba* L (Wang et al., 2017).

Surprisingly, with activity evaluation, alkaloids from MF had a good lipid-lowering effect, and significantly regulate the expression of key target proteins (PCSK 9 and LDL-R). Based on literature reported, PCSK9 is a serine protease known primarily in relation to its crucial function in low-density

lipoprotein (LDL) metabolism. After being secreted by the liver, PCSK9 binds to LDLR on hepatocyte surface and induces its degradation by directing its passage to the lysosomes. By promoting the degradation of LDL receptor (LDL-R) in hepatocytes, PCSK9 plays a crucial role in the regulation of plasma LDL cholesterol (LDL-C) concentrations (Cesaro et al., 2020; Dixon et al., 2016; Seidah and Garcon, 2022). The above effects led to the development and clinical application of new lipid-lowering drugs for PCSK9, namely alirocumab and evolocumab, respectively. Therefore, in the future, such alkaloids can be further obtained by separation, purification or synthesis. And related action mechanism research about these alkaloids can be carried out around two key proteins of PCSK9 and LDL-R, providing experimental basis for drug development to treat obesity and hyperlipidemia.

## 5. Conclusion

In this study, an integrated strategy with chemical characterization, *in vivo* metabolism, chemical isolation, and activity evaluation was established to systematically characterized and discover potential *in vivo* effective substances and *Mori Fructus* was used as an example. As a result, 72 constituents were characterized in MF. After oral administration of MF extract, 16 prototypes and 33 metabolites were rapidly identified. Among them, alkaloids with MS high response *in vitro* and *in vivo* were discovered, but their structures could not be confirmed because of various isomers and no reference standards. Immediately, six alkaloids (morusinic acid A-D, G, F) were isolated and identified by using various modern chromatographic methods and NMR techniques. Moreover, four alkaloids (morusinic acid A, morusinic acid B, morusinic acid F and morusinic acid G) had significant lipid-lowering activities with reducing triglyceride levels in fructose-induced HepG2 cell. With western blot experiment, they could play an important role in the lipid-lowering activity by down-regulating the expression of PCSK9 and promoting the expression of LDL-R in high-fructose-induced HepG2 cells. Our work provided meaningful information for revealing the potential active ingredients of MF in treatment of obesity and hyperlipidemia as well as quality control, and provided new ideas for exploring the *in vivo* effective substances in the complex system of TCM.

## CRedit authorship contribution statement

**Xi-yang Tang:** Conceptualization, Supervision, Methodology, Project administration, Writing – original draft, Writing – review & editing. **Peng-cheng Zhao:** Investigation, Validation, Writing – original draft. **Ming-hao Chen:** Investigation, Validation, Data curation. **Xiao-xing Wang:** Visualization, Investigation. **Cai-lian Fan:** Investigation, Data curation, Methodology. **Zhi-hong Yao:** Resources. **Xin-sheng Yao:** Resources. **Yi Dai:** Conceptualization, Methodology, Supervision, Project administration, Writing – review & editing.

## Declaration of Competing Interest

The authors declare that they have no known competing financial interests or personal relationships that could have appeared to influence the work reported in this paper.

## Acknowledgments

The present study was supported by Innovation Team and Talents Cultivation Program of National Administration of

Traditional Chinese Medicine (ZYYCXU-D-202203), National Natural Science Foundation of China (82204582), Science and Technology Projects in Guangzhou (202201010484) and Scientific Research Foundation for the introduction of talent of Pingdingshan University (PXY-BSQD2022040). We are grateful to Guangdong Tai'an-tang Pharmaceutical Co., Ltd. for providing *Mori Fructus*.

## Appendix A. Supplementary material

Supplementary data to this article can be found online at <https://doi.org/10.1016/j.arabjc.2023.104858>.

## References

- Asano, N., Oseki, K., Tomioka, E., Kizu, H., Matsui, K., 1994. N-Containing sugars from *Morus-Alba* and their glycosidase inhibitory activities. *Carbohydr. Res.* 259, 243–255.
- Asano, N., Yamashita, T., Yasuda, K., Ikeda, K., Kizu, H., Kameda, Y., Kato, A., Nash, R.J., Lee, H.S., Ryu, K.S., 2001. Polyhydroxylated alkaloids isolated from mulberry trees (*Morus alba* L.) and silkworms (*Bombyx mori* L.). *J. Agric. Food Chem.* 49, 4208–4213.
- Bian, L., Chen, H.G., Gong, X.J., Zhao, C., Zhou, X., 2021. *Mori Fructus* polysaccharides attenuate alcohol-induced liver damage by regulating fatty acid synthesis, degradation and glycerophospholipid metabolism in mice. *Front. Pharmacol.*, 12.
- Cao, H., Ji, W., Liu, Q., Li, C., Huan, Y., Lei, L., Fu, Y., Gao, X., Liu, Y., Liu, S., Shen, Z., 2021. *Morus alba* L. (Sangzhi) alkaloids (SZ-A) exert anti-inflammatory effects via regulation of MAPK signaling in macrophages. *J. Ethnopharmacol.* 280, 114483.
- Cesaro, A., Bianconi, V., Gragnano, F., Moscarella, E., Fimiani, F., Monda, E., Scudiero, O., Limongelli, G., Pirro, M., Calabro, P., 2020. Beyond cholesterol metabolism: The pleiotropic effects of proprotein convertase subtilisin/kexin type 9 (PCSK9). *Genetics, mutations, expression, and perspective for long-term inhibition. Biofactors* 46, 367–380.
- Chan, E.W.C., Lye, P.Y., Wong, S.K., 2016. Phytochemistry, pharmacology, and clinical trials of *Morus alba*. *Chin J. Nat. Medicines* 14, 17–30.
- Chen, Z., Du, X., Yang, Y., Cui, X., Zhang, Z., Li, Y., 2018. Comparative study of chemical composition and active components against alpha-glucosidase of various medicinal parts of *Morus alba* L. *Biomed. Chromatography : BMC* 32, e4328.
- Czechowski, T., Weathers, P.J., Brodelius, P.E., Brown, G.D., Graham, I.A., 2020. Editorial: artemisinin-from traditional Chinese medicine to artemisinin combination therapies; four decades of research on the biochemistry, physiology, and breeding of *Artemisia annua*. *Front. Plant Sci.* 11.
- Dixon, D.L., Trankle, C., Buckley, L., Parod, E., Carbone, S., Van Tassel, B.W., Abbate, A., 2016. A review of PCSK9 inhibition and its effects beyond LDL receptors. *J. Clin. Lipidol.* 10, 1073–1080.
- Do, H.J., Chung, J.H., Hwang, J.W., Kim, O.Y., Lee, J.Y., Shin, M.J., 2015. 1-Deoxynojirimycin isolated from *Bacillus subtilis* improves hepatic lipid metabolism and mitochondrial function in high-fat-fed mice. *Food Chem. Toxicol.* 75, 1–7.
- Du, K.Z., Chen, Y., Li, J., Tian, F., Gao, X.M., Chang, Y.X., 2019. Determination of antioxidant ingredients in *Mori Fructus* employing ionic liquid-assisted miniaturized matrix solid-phase dispersion extraction via ultra-performance liquid chromatography. *J. Food Biochem.* 43.
- He, X.R., Fang, J.C., Ruan, Y.L., Wang, X.X., Sun, Y., Wu, N., Zhao, Z.F., Chang, Y., Ning, N., Guo, H., Huang, L.H., 2018. Structures, bioactivities and future prospective of polysaccharides from *Morus alba* (white mulberry): a review. *Food Chem.* 245, 899–910.

- Hong, Y., Mitchell, A.E., 2004. Metabolic profiling of flavonol metabolites in human urine by liquid chromatography and tandem mass spectrometry. *J. Agric. Food Chem.* 52, 6794–6801.
- Hou, X.M., Zhang, C.X., Wang, L.M., Wang, K.W., 2021. Natural piperine improves lipid metabolic profile of high-fat diet fed mice by upregulating SR-B1 and ABCG8 transporters. *J Nat Prod* 84, 373–381.
- Jelled, A., Ben Hassine, R., Thouri, A., Flamini, G., Chahdoura, H., El Arem, A., Ben Lamine, J., Kacem, A., Haouas, Z., Ben Cheikh, H., Achour, L., 2017. Immature mulberry fruits richness of promising constituents in contrast with mature ones: a comparative study among three Tunisian species. *Ind. Crop Prod.* 95, 434–443.
- Kang, K.B., Park, E.J., da Siva, R.R., Kim, H.W., Dorrestein, P.C., Sung, S.H., 2018. Targeted isolation of neuroprotective dicoumaroyl neolignans and lignans from *Sageretia theezans* using in silico molecular network annotation propagation-based dereplication. *J. Nat. Prod.* 81, 1819–1828.
- Kusano, G., Orihara, S., Tsukamoto, D., Shibano, M., Coskun, M., Guvenc, A., Erdurak, C.S., 2002. Five new nortropane alkaloids and six new amino acids from the fruit of *Morus alba* LINNÉ growing in Turkey. *Chem. Pharm. Bull.* 50, 185–192.
- Lim, S.H., Choi, C.I., 2019. Pharmacological Properties of *Morus nigra* L. (Black Mulberry) as A Promising Nutraceutical Resource. *Nutrients*, 11.
- Ma, G.Q., Chai, X.Y., Hou, G.G., Zhao, F.L., Meng, Q.G., 2022. Phytochemistry, bioactivities and future prospects of mulberry leaves: a review. *Food Chem* 372.
- Majolo, F., Delwing, L.K.D.B., Marmitt, D.J., Bustamante, I.C., Goettert, M.I., 2019. Medicinal plants and bioactive natural compounds for cancer treatment: Important advances for drug discovery. *Phytochem. Lett.* 31, 196–207.
- Mi, N., Cheng, T.F., Li, H.L., Yang, P.M., Mu, X.M., Wang, X.Y., Zu, X.P., Qi, X.P., Guo, X., Ye, J., Zhang, W.D., 2019. Metabolite profiling of traditional Chinese medicine formula Dan Zhi Tablet: an integrated strategy based on UPLC-QTOF/MS combined with multivariate statistical analysis. *J. Pharmaceut Biomed.* 164, 70–85.
- Musunuru, K., Chadwick, A.C., Mizoguchi, T., Garcia, S.P., DeNizio, J.E., Reiss, C.W., Wang, K., Iyer, S., Dutta, C., Clendaniel, V., Amaonye, M., Beach, A., Berth, K., Biswas, S., Braun, M.C., Chen, H.M., Colace, T.V., Ganey, J.D., Gangopadhyay, S.A., Garrity, R., Kasiewicz, L.N., Lavoie, J., Madsen, J.A., Matsumoto, Y., Mazzola, A.M., Nasrullah, Y.S., Nneji, J., Ren, H., Sanjeev, A., Shay, M., Stahley, M.R., Fan, S.H.Y., Tam, Y.K., Gaudelli, N.M., Ciaramella, G., Stolz, L.E., Malyala, P., Cheng, C. J., Rajeev, K.G., Rohde, E., Bellinger, A.M., Kathiresan, S., 2021. In vivo CRISPR base editing of PCSK9 durably lowers cholesterol in primates. *Nature* 593, 429.
- Newman, D.J., Cragg, G.M., 2016. Natural products as sources of new drugs from 1981 to 2014. *J. Nat. Prod.* 79, 629–661.
- Ou, T.T., Hsu, M.J., Chan, K.C., Huang, C.N., Ho, H.H., Wang, C.J., 2011. Mulberry extract inhibits oleic acid-induced lipid accumulation via reduction of lipogenesis and promotion of hepatic lipid clearance. *J. Sci. Food Agric.* 91, 2740–2748.
- Ou-yang, Z., Cao, X., Wei, Y., Zhang, W.W.Q., Zhao, M., Duan, J.A., 2013. Pharmacokinetic study of rutin and quercetin in rats after oral administration of total flavones of mulberry leaf extract. *Rev. Bras Farmacogn.* 23, 776–782.
- Petroglou, D., Kanellos, I., Savopoulos, C., Kaiafa, G., Chrysochoou, A., Skantzis, P., Daios, S., Hatzitolios, A.I., Giannoglou, G., 2020. The LDL-Receptor and its molecular properties: from theory to novel biochemical and pharmacological approaches in reducing LDL-cholesterol. *Curr. Med. Chem.* 27, 317–333.
- Seidah, N.G., Garcon, D., 2022. Expanding biology of PCSK9: roles in atherosclerosis and beyond. *Curr Atheroscler Rep* 24, 821–830.
- Setzer, W.N., Setzer, M.C., Bates, R.B., Jackes, B.R., 2000. Biologically active triterpenoids of *Syncarpia glomulifera* bark extract from Paluma, north Queensland, Australia. *Planta Med* 66, 176–177.
- Song, D.X., Jiang, J.G., 2017. Hypolipidemic components from medicine food homology species used in China: pharmacological and health effects. *Arch. Med. Res.* 48, 569–581.
- Tang, X.Y., Zeng, J.X., Dai, Z.Q., Chen, M.H., Ye, M.N., Yao, Z.H., Dai, Y., Yao, X.S., 2020. Identification and characterization of chemical constituents in Qi-Lin pills and their metabolites in rat bio-samples after oral administration using ultra-high performance liquid chromatography with quadrupole time-of-flight mass spectrometry. *J. Pharmaceut Biomed.* 188.
- Tsudoku, T., Nakamura, Y., Honma, T., Nakagawa, K., Kimura, T., Ikeda, I., Miyazawa, T., 2009. Intake of 1-Deoxyojirimycin suppresses lipid accumulation through activation of the beta-oxidation system in rat liver. *J. Agric. Food Chem.* 57, 11024–11029.
- Wang, N.N., Zhu, F.F., Chen, K.P., 2017. 1-Deoxyojirimycin: sources, extraction, analysis and biological functions. *Nat. Prod. Commun.* 12, 1521–1526.
- Wani, M.C., Taylor, H.L., Wall, M.E., Coggon, P., McPhail, A.T., 1971. Plant antitumor agents. VI. The isolation and structure of taxol, a novel antileukemic and antitumor agent from *Taxus brevifolia*. *J. Am. Chem. Soc.* 93, 2325–2327.
- Wu, T., Qi, X., Liu, Y., Guo, J., Zhu, R., Chen, W., Zheng, X., Yu, T., 2013. Dietary supplementation with purified mulberry (*Morus australis* Poir) anthocyanins suppresses body weight gain in high-fat diet fed C57BL/6 mice. *Food Chem.* 141, 482–487.
- Wu, M.J., Wu, X.L., Zhang, D.Q., Qiu, F., Ding, L.Q., Ma, H.L., Chen, X.Z., 2017. Metabolic profiling of quercetin in rats using ultra-performance liquid chromatography/quadrupole-time-of-flight mass spectrometry. *Biomed. Chromatogr.* 31.
- Yang, W.Z., Zhang, Y.B., Wu, W.Y., Huang, L.Q., Guo, D., Liu, C. X., 2017. Approaches to establish Q-markers for the quality standards of traditional Chinese medicines. *Acta Pharm. Sin. B* 7, 439–446.
- Yuan, R., Lin, Y., 2000. Traditional Chinese medicine: an approach to scientific proof and clinical validation. *Pharmacol. Therapeut.* 86, 191–198.
- Yuan, Q.X., Zhao, L.Y., 2017. The Mulberry (*Morus alba* L.) Fruit-A Review of Characteristic Components and Health Benefits. *J. Agric. Food Chem.* 65, 10383–10394.
- Zhang, T.J., Bai, G., Han, Y.Q., Xu, J., Gong, S.X., Li, Y.Z., Zhang, H.B., Liu, C.X., 2018b. The method of quality marker research and quality evaluation of traditional Chinese medicine based on drug properties and effect characteristics. *Phytomedicine: Int. J. Phytotherapy Phytomedicine.* 44, 204–211.
- Zhang, J.Q., Li, C., Huang, Q., You, L.J., Chen, C., Fu, X., Liu, R.H., 2019b. Comparative study on the physicochemical properties and bioactivities of polysaccharide fractions extracted from *Fructus Mori* at different temperatures. *Food Funct.* 10, 410–421.
- Zhang, F.X., Li, Z.T., Li, M., Yuan, Y.L.L., Cui, S.S., Chen, J.X., Li, R.M., 2021. Dissection of the potential anti-influenza materials and mechanism of *Lonicerae japonicae* flos based on in vivo substances profiling and network pharmacology. *J. Pharmaceut Biomed.* 193.
- Zhang, L., Shen, H., Xu, J., Xu, J.D., Li, Z.L., Wu, J., Zou, Y.T., Liu, L.F., Li, S.L., 2018a. UPLC-QTOF-MS/MS-guided isolation and purification of sulfur-containing derivatives from sulfur-fumigated edible herbs, a case study on ginseng. *Food Chem.* 246, 202–210.
- Zhang, A.H., Sun, H., Yan, G.L., Han, Y., Zhao, Q.Q., Wang, X.J., 2019a. Chinmedomics: a powerful approach integrating metabolomics with serum pharmacochemistry to evaluate the efficacy of traditional Chinese medicine. *Engineering-Prac* 5, 60–68.
- Zhao, W.Y., Shang, X.Y., Zhao, L., Yao, G.D., Sun, Z., Huang, X.X., Song, S.J., 2018. Bioactivity-guided isolation of beta-Carboline alkaloids with potential anti-hepatoma effect from *Picrasma quassioides* (D. Don) Benn. *Fitoterapia* 130, 66–72.
- Zhou, X.D., Tang, L.Y., Xu, Y.L., Zhou, G.H., Wang, Z.J., 2014. Towards a better understanding of medicinal uses of *Carthamus tinctorius* L. in traditional Chinese medicine: a phytochemical and pharmacological review. *J. Ethnopharmacol.* 151, 27–43.